University of South-Eastern Norway

www.usn.no

FMH606 Master's Thesis 2022

Process Technology

Application of autonomous inflow control valve for enhanced bitumen recovery by steam assisted gravity drainage

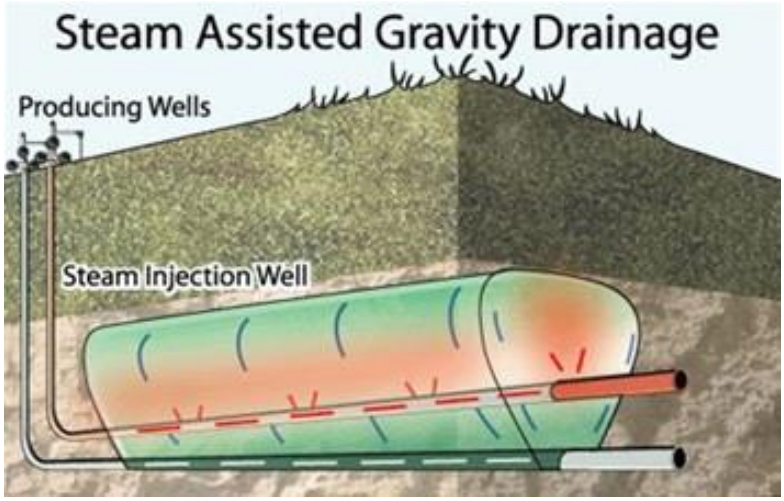

Farzan Farsi Madan

Faculty of Technology, Natural sciences and Maritime Sciences

Campus Porsgrunn

University of South-Eastern Norway

www.usn.no

Course: FMH606 Master's Thesis, 2022

Title: Application of autonomous inflow control valve for enhanced bitumen recovery by steam assisted gravity drainage

Number of pages: 44

Keywords: steam assisted gravity drainage, enhanced oil recovery, non-condensable gases, autonomous inflow control valve, steam to oil ratio, gas liquid ratio, near well simulation, OLGA/ROCX.

Student: Farzan Farsi Madan

Supervisor: Britt Moldestad, Soheila Taghavi Hosnaroudi

External partner: InflowControl AS

Summary:

Production of bitumen through the thermal process, SAGD, is of interest since the warmed bitumen can be easily produced by aid of gravity towards the horizontal production wells. This approach beside its advantages has its own draw-back.

One of these disadvantages is the breakthrough of steam and gas from the reservoir into the production well. ICDs are the simplest form of an inflow control device to delay the inflow of the unwanted gas. These devices are quite cheap but when it comes to the functionality, they show a poor performance in chocking the gas inflow.

autonomous inflow control valves (acronymized as AICV), are the modern inflow controllers which can closely measure the gas and water content of an inflow stream and partially or fully open and close the valve to mitigate the trace of water and gas in the produced bitumen flow.

In this thesis, basic theory around the thermal production of the bitumen is provided as well as the comparison of capability of these two inflow control technologies from different perspectives.

Preface

In this master thesis, ICD and AICV, the major inflow control technologies in controlling of bitumen production wells were closely investigated by the help of simulated data from OLGA simulator. This thesis was conducted at University of South-Eastern Norway in Spring semester 2022.

External partner which aided this project with its long-term experience in the oil production industry was InflowControl AS, whose main focus is on the design of the autonomous inflow control valves (AICV) for various oil fields.

On the path of preparation of this research, I was lucky to have an experienced and amazing supervising team. I want to thank my supervisor, Professor Britt Moldestad for her great encouragements along the way and her energy and patience. I am also very thankful to my great co-supervisor, Soheila Taghavi Hosnaroudi from InflowControl AS, who nourished my knowledge about the horizontal oil production, challenges and solutions at hand in this industry. Also, I want to thank Ramesh Timsina, whose guidance for OLGA simulation tool was really helpful. I am deeply thankful to this team, because of their patience and the extraordinary energy that they gave me in the whole semester.

Last but not least, my family, the great construction in which I was provided with the fantastic enthusiasm and inspiration to conduct this piece of research.

Thank you!

Porsgrunn, 25.05.2022

Farzan Farsi Madan

Contents

Figures overview

Tables overview

Nomenclature

Symbol	Unit	Definition
Re	-	Reynolds number
P	Pa	Pressure
μ	cP	Viscosity
C_D	-	Drag coefficient
D	m	Diameter
L	m	Length
A	m	Flow cross-sectional area
ϕ	-	Porosity
k	D or mD	Absolute permeability
k_f	D or mD	Effective permeability of fluid f
k_{rf}	-	Relative permeability of fluid f
K_{rgom}	-	maximum value of relative permeability of gas at its maximum saturation in an oil-gas reservoir
k_{rowc}	-	the maximum value of relative permeability of oil at its maximum saturation in the presence of water at irreducible water saturation
S_{wc}	-	irreducible water saturation
n	-	Correy exponent

1. Introduction

Fossil fuels such as oil and gas have been one of the greatest demands of the human society for decades; Transportation, construction, heating purposes, manufacturing and electricity production are just some of the applications of the fossil fuels. As we know, fossil fuels are generated via natural procedures of which take place slowly, at a very slow pace incomparable to the consumption rate of these valuable materials. Thus, mankind must be more considerate towards the current amount of oil and gas existing in the globe. Since oil is day by day getting more demanded in the global market and this is mainly due to the growth of global population, the number of oil reservoirs which can be excavated by conventional methods are reducing. As the resultant, recovery methods, both secondary and tertiary are introduced to recover more oil at the reservoirs which are already given up on primary or conventional oil production methods.

Steam-assisted gravity drainage (SAGD) process is one these tertiary or enhanced oil recovery (EOR) methods which is nowadays being used in America and Canada for higher oil recovery.

This thermal process is devised simply to reduce to viscosity of the oil, mainly heavy and extra-heavy oil types like bitumen, in order to help the flow of the oil to the production well.

Producing the oil that is reserved in a reservoir along with gas and water is not challenge-free operation since producing oil also provokes the gas and water stored in the operating reservoir to leak to the production well. ICDs and AICVs are the solution to these unwanted leakages. These inflow control devices delay or choke the incoming gas or water.

In this research, an explanation on the SAGD thermal method and investigation of the two major inflow control technologies (ICD and AICV), as well as the demonstration of their functionalities will be provided. For obtaining reliable data which gives us adequate insight for comparisons, the simulation tool OLGA was used, which is a dynamic multiphase flow, flowline and pipeline simulator that works in combination with its robust add-on, ROCX, the near-wellbore reservoir simulator, which helps us to create a unique and fully customized reservoir with its properties.

1.1 Study background

Bitumen is a high-viscous oil type whose thermal production gained popularity in the late 90's. Water and gas breakthrough is an inevitable challenge of any horizontal-well production. Therefore, various type of inflow control technologies has been devised and deployed to reduce the gas production. Development of controllers started with the most basic type, ICD controllers, and ends up to the most advanced controller, AICV.

This technology has been applied to many production fields, with different initial multi-phase saturations, since it is quite reliable piece of instrument to avoid water and gas breakthrough, even in situations where the product (oil) has the same viscosity as the water.

1.2 Outline

In the upcoming chapters, the bitumen is set as the main recovery product, go through the SAGD process and its profits and challenges, introduce and explain the inflow control devices, run near-well based simulations by help of the OLGA software and sit and observe the results of the simulations and explain the privileges and drawbacks of the two main inflow control devices, the ICD and AICV, and their contribution in improving the efficiency of the SAGD process as well as a conclusion on the research case.

2. Literature review

In this chapter, an introductory presentation of the bitumen is given as well as a look into the tertiary thermal recovery processes, mainly SAGD. In addition, a brief comparison of the main thermal recovery methods will be provided.

2.1. Bitumen

Bitumen is a semi-solid form of petroleum that is composed of the hydrocarbons such as resins, asphaltenes and PAHs (polycyclic aromatic hydrocarbons). Although such compounds are found in lighter oil types but they are significantly concentrated in the bitumen structure, which is the main reason of categorizing the bitumen as one of the least-viscous crude oils [1]. Bitumen has five main grade types and with considering the physical properties, these variations of bitumen are applied in construction industry (paving and roofing), as a binder in asphalt, soundproofing and explosives [2].

Athabasca oil sands are the greatest supply of the bitumen which are located in Alberta, Canada. An area of roughly 140,000 km^2 is the gigantic work area for the companies like Syncrude Canada Ltd., Suncor Énergie and Nexen where they produce the natural bitumen at a rate of 2.8 million barrels per day. [3]

Generally, in oil and bitumen recovery, there are three levels of recovery of which production engineers apply in order to extract as much oil as the reservoirs allow. Primary recovery is simply performed by help of the initial pressure of the reservoir which pushes the oil toward the production well and eventually to the surface. Secondary recovery come handy when the initial pressure falls below the limit and the oil is not able anymore to flow through the path to the ground surface. Gas or water is injected in as a compensation to the pressure drop and this causes the oil to flow through the rock and flow towards the production well [4]. Since primary and secondary recovery methods recover only 20 to 40 percent of the original oil in place [5], enhanced or tertiary recovery methods are required to increase the production from a reservoir. Enhanced recovery methods come to play when neither the reservoir pressure is enough to lift the oil to the ground surface (primary method) nor the injection of oil or water is able to displace the remaining bitumen, here tertiary or enhanced methods step in and get hailed as a milestone in bitumen production. Unlike the primary and secondary methods where pressure gradient is the only lever of increasing the bitumen recovery, the enhanced recovery methods increase the mobility of the bitumen via changing the physical properties, mainly the bitumen viscosity. Bitumen, known as the heaviest type of oil, with an API of roughly equal to $8°$ (less than $10°$ as an extra-heavy oil) has a very high viscosity (greater than $5x10^5$ cP at 25 $°C$) [6] and this viscosity is high enough to resist the bitumen flow towards the surface specially when the pressure in the reservoir is dropped below the required level.

2.2. Thermal processes

As said before, tertiary methods (EOR) are used after the primary and secondary methods cannot drive the oil out of the reservoir therefore, changing oil properties is seemingly the best solution to increase the recovery. Tertiary methods are only applied to the reservoirs, where the oil laying underneath the surface, is valuable enough to operate the expensive tertiary

methods. Bitumen, as explained before, is a very heavy oil but should not be judged by its high density as a low-grade component, this oil is being used as one of the most beneficial consumables in the world.

There are three main tertiary method that are being used as the current technology which are known as: gas injection, chemical injection and thermal injection. Thermal injection method has been done so far by either use of the steam thermal energy in order to heat up the bitumen or as the second alternative, burning a part of the bitumen to heat up the remaining of the reserved bitumen (fire flooding); of which both result in a less viscous bitumen and an increase in the oil production [4].

Going deeper in the thermal or steam injection methods, we find three alternatives of recovery [7]:

a) Steam flooding

This method that is being used by companies (e.g., Chevron Corporation) is carried simply by injecting hot steam into a vertical well, the injected steam basically warms up a heavy oil (e.g., bitumen). The colder steam rises through the same well that was injected previously while the warmed-up bitumen that now has a lower viscosity, rises up towards the surface through a vertical well drilled parallel to the steam injection wellbore. [8]

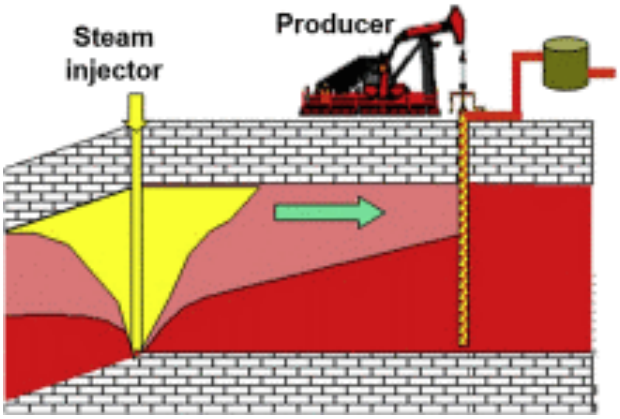

Figure 2-1: Steam flooding [9]

The advantage of steam flooding to its counterpart method (fire flooding) is that it is easier to control and due to lower operating temperature (compared to fire flooding), it does not generate environment threatening gases (by cracking of the oil) [10].

b) Cyclic steam simulation (CSS or huff and puff)

This method is another in-situ recovery method that is applied to recover bitumen at the depth of approximately 400 to 600 meters under the surface. This operation is basically consisted of three main stages, injection, soak and production stage. These three stages of recovery are done respectively in a way that first a vertical hole is drilled then steam is injected in the formation to warm up the bitumen, after a time that the bitumen

absorbed the energy of the steam (soak stage), then the bitumen starts to be produced towards the surface (production stage) [11].
This method has its up and down sides, one of the advantages to this method is that all the recovery cycle (injection-soak-production) is just carried on by one well and therefore there is no need to drill more than one wellbore which consequently helps to a lower capital investment [12]. On the other hand, one of the drawbacks of this method is that there must be a one-month time gap between the injection and production stage (soak stage), so the injected steam has enough time to deliver the desired heat to the bitumen and eventually the injection well be prepared to be used as a production well [13].

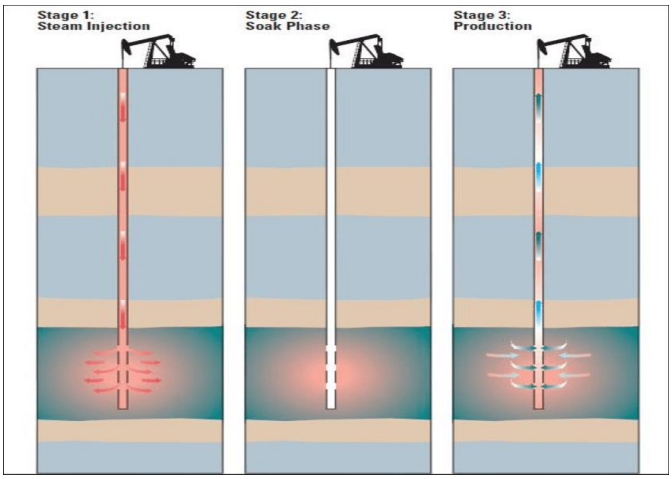

Figure 2- 2: Cyclic steam simulation [14]

c) Steam Assisted Gravity Drainage (SAGD)

SAGD or the steam assisted gravity drainage, was first devised by Dr. Roger Butler (1927-2005), who was an engineer at the Imperial Oil petroleum company [15].
He was sent to Alberta to conduct research on bitumen recovery and his researches led to this idea; drill two horizontal well down in the depth of up to 800 meters, warm up the bitumen by injecting steam into the vertical end of one of the wells and produce the bitumen via another vertical end on the second well [16].

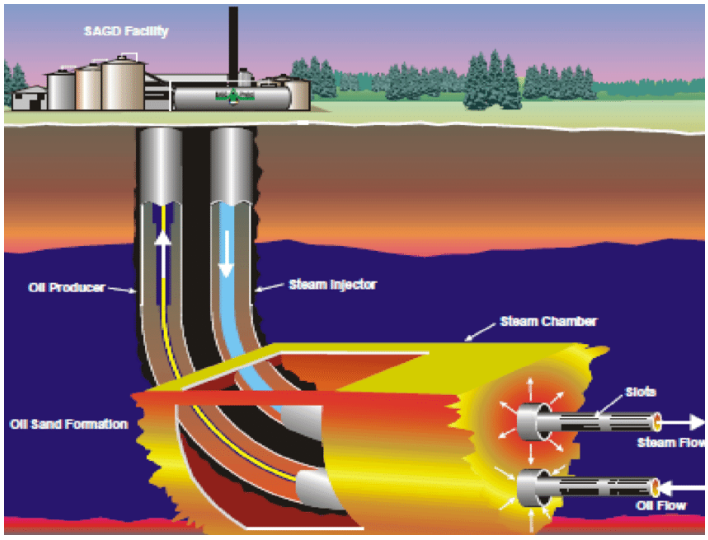

Figure 2- 3: SAGD process [17]

Cenovus Energy was the first company to run a whole commercial project (named project Foster Creek) by aid of this in-situ recovery method between 1997 and 2001. Bitumen that was produced in this project, was laying under the surface at a depth of 450 meters [18]. Note that, SAGD process was mainly invented in order to produce heavy oil types like bitumen, which are trapped under a caprock where either it was too deep or too difficult to access by preceding thermal methods [19]. This company also conducted Christina Lake project (bitumen at a depth of 375 meters) and Sunrise project (bitumen at a depth of 200 meters), all of which, were the first commercial projects to produce bitumen using the SAGD in the history of the oil production [18].
In SAGD, the distance between the injection well and production well (each with a length of 1000 meters) is normally from five up to ten meters. In order to kick start the SAGD in a more efficient way, the steam is injected for one up to three months into the both injection and production well to give an acceptable motion to the bitumen so it can be dragged down towards the production well by the gravity forces, after this time, steam will be only injected via the injection well.

Along with the bitumen, water and gas in the reservoir tend to enter the production well and consequently emerge in the final extraction product which is absolutely not favorable since it incurs both capital and operational costs for downstream sectors.

In order to avoid or mitigate the unwanted water and gas content, inflow control devices are designed and installed on the well to disturb the water and gas breakthrough, water and gas coning and sand production [20]. These devices do not have the capability of blocking the water and gas flow towards the production well but they just delay their inflow. In order to take more control on gas and water breakthrough, designers have invented a more intelligent generation of inflow controllers which are introduced as AICV. These intelligent pieces of equipment are able to choke 90% or more of water and gas which are trying to overtake the oil inflow. The key success to such gas and water breakthrough avoidance is the detection of density and viscosity differentials which exists between oil, water and gas [21].

2.3. Inflow control technologies

Producing water and gas along with the main production material which is oil, is unfavored for downstream sectors. This issue showed its significance where the oil recovery industry started to use the horizontal wells. Producing oil from a horizontal well has its up and down sides, the greatest advantage of using horizontal wells is that a larger area in a reservoir gets into contact with the production wellbore and consequently increases the oil production from the reservoir. One of the challenges that exists in such oil recovery (horizontal wells) is heel-to-toe effect. The oil flowing through a horizontal well, due to the friction with the well boundaries, loses its pressure along the well length, from the toe to heel. Therefore, the pressure drop at the heel section gets a higher than the pressure drops at the toe section (longer horizontal wells have stronger heel-to-toe effect). As a result, in oil production from a horizontal well, the area of the reservoir that is in proximity to the heel section of well, gets drained quicker from the oil than the toe section (due to the lower pressure in the well at the heel) and therefore water and gas start to enter via these sections (water and gas coning), in order to avoid such undesired situation, ICDs were invented and used in early 1990's [22].

Here, two important inflow control technologies are described, first ICDs, as the pioneers to the water and gas breakthrough avoidance and next, AICVs, the newest technology at hand to minimize the production of the unwanted water and gas.

a) Inflow control devices (ICDs)

Inflow control devices or ICDs can be installed along a horizontal well in order to create pressure drop via either friction or density. They are relatively cheap inflow control devices and do not require any control from the ground surface, once get installed in the desired depth, they start and keep on working based on their initial design, due to this fact they are also called passive inflow control devices.

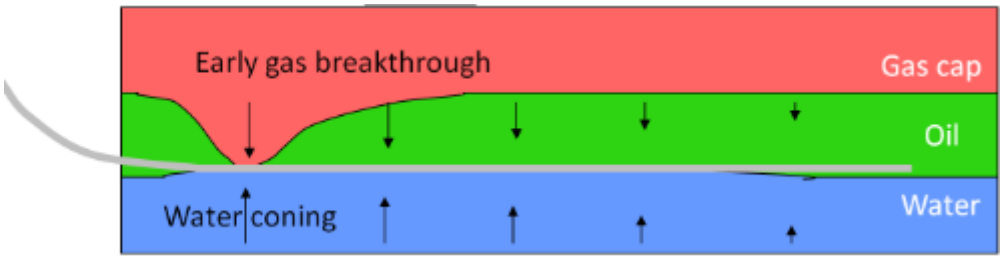

Figure 2-4: gas breakthrough (no ICD) [23]

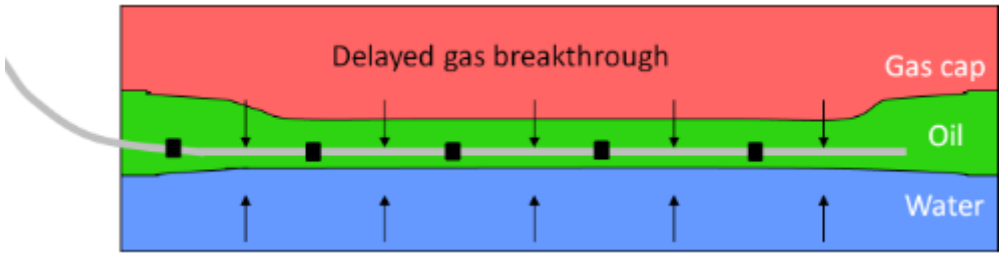

Figure 2-5: gas breakthrough (installed ICDs) [23]

ICDs which use the friction to generate pressure drop are called channel type ICD. Channel type control devices basically allow the inflow stream to enter a set of screens towards the base-pipe. After flowing through the screens and entering the base pipe, the fluid crosses the annulus of the well in a helical pattern and then pours into the main production well. Since the fluid changes its flow direction several times during its travel and as a matter of fact, the alloy used to manufacture the multi-layered screens and helical passage is not completely smooth and has a roughness value of lower than one, exerts a friction force against the fluid flow direction and this eventually generates the desired pressure drop required to delay the water breakthrough. The key to the design of the channel type ICDs is defining the length and diameter of the channels which cannot be adjusted after being installed under the ground [20].

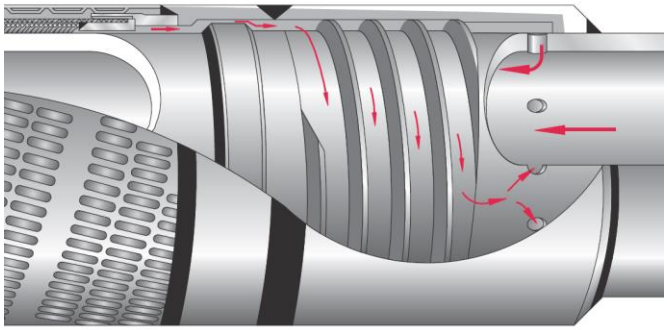

Figure 2-6: Channel type ICD [24]

Another type of inflow control device is called orifice type ICD. The function is very simple, flow resistance occurs when fluid tries to enter the orifice/nozzle openings installed on the reservoir base pipe. Unlike the channel type ICDs, the orifice ICD functions based on density differences (density sensitive ICD), which means that instead of altering the flow direction of the incoming inflow stream to obtain the pressure drop (channel type), it generates the desired pressure drop via squeezing the fluid flow through an orifice, this can be easily explained by the Bernoulli's equation [20].

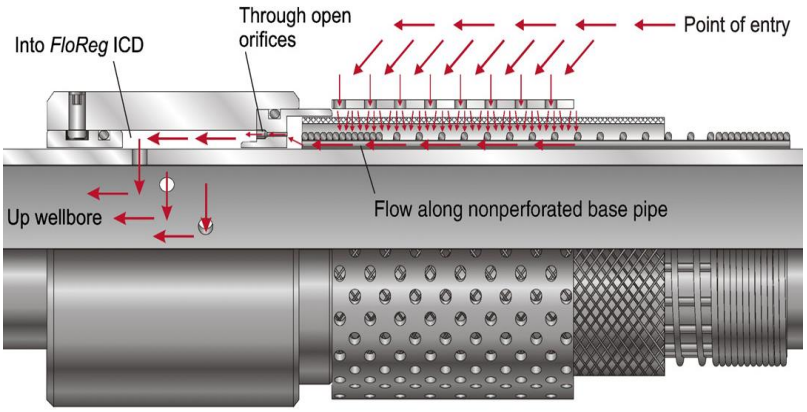

Figure 2-7: Orifice type ICD [24]

This type is more commonly used ICD compared to the channel type since this ICD type is the simplest in design, is efficient in water-choking due to its functionality based on density not friction and also very beneficial when the viscosity difference of oil and water is quite alternating [25]. Orifice ICD can have nozzles as small as a diameter of approximately 3.18 mm and are mainly made of tungsten carbide, one of most rigid materials at hand [26].

b) Autonomous Inflow control valves (AICVs)

ICDs have considerable disadvantages, first, they are not adjustable, once designed and installed, they cannot be adjusted to accommodate to the dynamic behavior of the reservoir, second, they are unable to choke the water or gas after the breakthrough happens [27]. Therefore, the need for an inflow control tool, which could cover the inabilities of ICDs started to be sensed. Eventually, AICVs, the newer generation of inflow control tools emerged into the oil production industry in year 2012. Prototypes were first designed by Norwegian company, InflowControl AS, then Saudi Aramco Energy Venture company invested on the technology one year after finally in year 2015, the first AICVs were installed offshore and deployed in GCC area (The Gulf Cooperation Council) [28].

An AICV, is an “autonomous” inflow control valve which unlike an ICD (passive device), is regarded as an “active” control system. In order to generate the required pressure drop, instead of using a simple non-moving orifice or channel, the AICV controls the inflow stream from the reservoir by a movable piston [21].

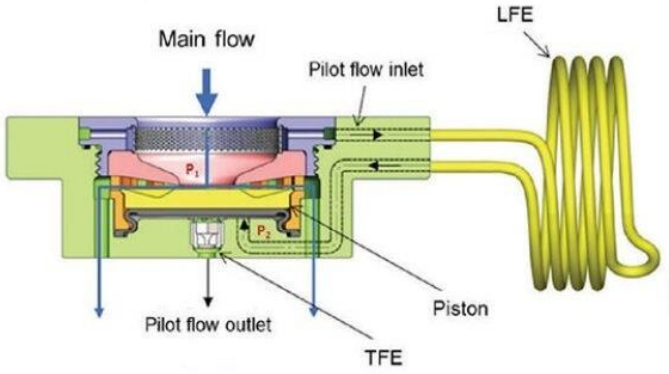

Figure 2-8: Schematic of an AICV [29]

When a fluid flow of either oil, water or gas tries to enter these valves, a small portion of the incoming fluid separates from the main stream and flows through the "mechanically smart" control section of the AICV system. Inside this control section, both the viscosity and the density of the flowing fluid causes the moving piston of the AICV to remain open or shut down. This brand-new technology has been used since the pilot project in GCC (in 2015) and has been deployed on over 170 wells containing light, medium and heavy oil types [30].

3. Theoretical background

In this chapter, first an explanation for the mathematical equations around the inflow control technologies introduced in the previous chapter (ICD and AICV) are given then, some general definitions required to understand the process of bitumen production will be also provided.

3.1. Inflow control device at a closer look

Here, in this research, the orifice type ICD is selected as a representative for the inflow control devices since this is the cheapest and the most widely used type of ICD.
An orifice ICD, as illustrated in figure 3-1, is basically formed of two parts, the nozzle and the housing. Base on equation 3-1 [31], a pressure drop of Δp is created when a fluid with ρ density is flowing through a cross section of A, at a volumetric flow rate of q_v [31].

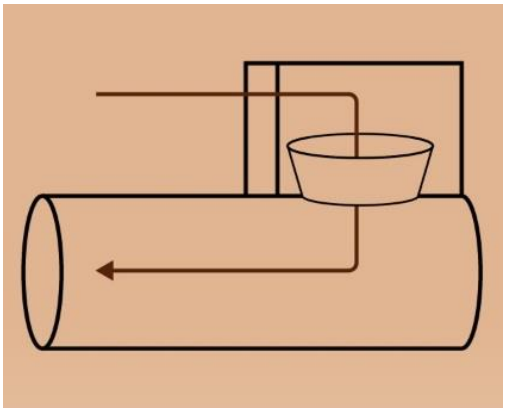

Figure 3-1: nozzle and housing [32]

$$\Delta p = \frac{\rho}{2}\left(\frac{q_v}{C_D \cdot A}\right)^2 \tag{3-1}$$

$$A = \frac{\pi \cdot D^2}{4} \tag{3-2}$$

C_D, is the drag coefficient, simply a value which shows the resistance of an object in a fluid flow.

In the analysis of a nozzle ICD, A is the opening of the nozzle, ρ can be density of oil, gas or water. When a fluid passes through the nozzle and the housing which is enclosing

the nozzle, due to unevenness of the nozzle and the housing, feels a drag force against the flow path (drag coefficient, C_D, is in the range of 0.8 and 0.97 based on the alloy being used in the ICD). This drag force based on the equation 3-1, causes a pressure drop in the flow of the incoming fluid [32].

In order to have a simpler handling of the inflow stream by the ICDs, manufacturers produce the body of the nozzle as rigid as possible (by usage of tungsten carbide as the main material) to keep the cross section area absolutely constant, that is why orifice ICD is better known as "density sensitive inflow controller" which means that the inflow to the production well is controlled by the difference in fluids densities, or in another words, volumetric flow rate of a fluid crossing an orifice ICD which is a function of the pressure drop, is solely depended to its density (equation 3-1) [31].

For example, compare two streams inflowing the nozzle ICD, one is water stream and the another one is oil stream. Based on equation 3-1, due to the higher density of the water compared to oil (ρ), the pressure drop is higher (Δp) and therefore the oil volumetric flow rate goes higher than water (q_v), which means a higher production of oil compared to water. This helped tremendously the recovery of oil in a water-drive reservoirs but, in the presence of gas, ICDs do not show a promising result [32]. Let us have closer look.

The performance curves below display the production of oil, water and from a well over time. The graph indicates that for a specific drawdown pressure difference (the driving force of an inflow from a reservoir into a production well), specific production flow rates for oil, water and gas can be calculated. For example, at a pressure difference of 30 bar, water is produced at flow rate of approximately 800 l/h, whereas at the same pressure difference, a higher flow rate of roughly 850 l/h is shown for the oil which means that the ICD control system is carrying out the job acceptably.

But by looking at the red curve which indicates the performance curve for the gas, it is realized that gas is produced at a significantly higher flow rate (q_g >>1600 l/h) at the same pressure difference (30 bar). This is the biggest disadvantage of ICDs application in a reservoir with gas content [32].

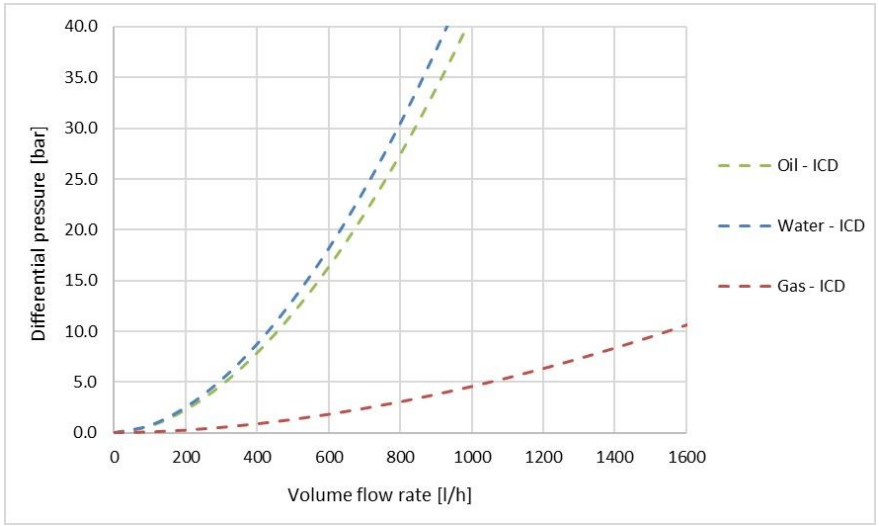

Figure 3-2: Performance curve [29]

3.2. Physics of an Autonomous inflow control valve

Unlike the ICDs that are regarded as “devices”, AICVs are not only a fixed structure with no moving part, they are quite active control instruments that can directly control the inflow to a production well, because of this behavior, they are referred as “valves” rather than “devices”. The reason why they are categorized as valves in oil industry is that within the body of an AICV, you can find a moving piston, which is the active part of the AICV (figure 3-3).

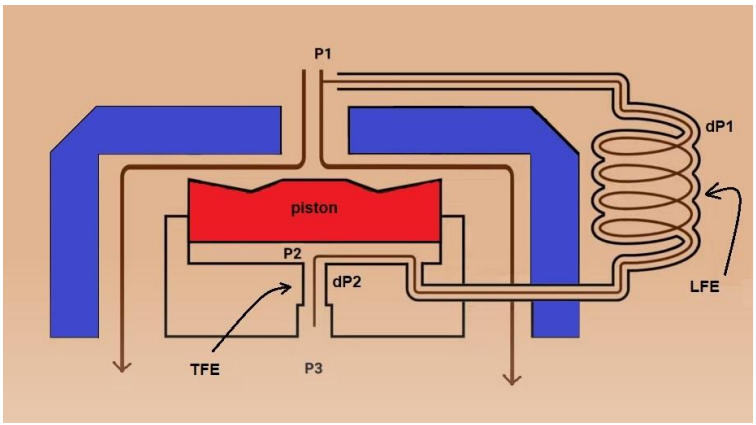

Figure 3-3: AICV schematic [33]

An AICV works based on both fluid density and fluid viscosity and this is closely managed by two main sections, the laminar flow element (LFE) and the turbulent flow element (TFE) (figure 3-3). Approximately, 3% of the fluid in the reservoir enters the LFE section as the pilot flow, here due to the constriction that the vessel dictates to the flowing fluid, in another words, the effect of the boundaries on the flow, the fluid feels an increasing pressure drop along the path within the LFE, growing with the length of the LFE (figure 3-4).

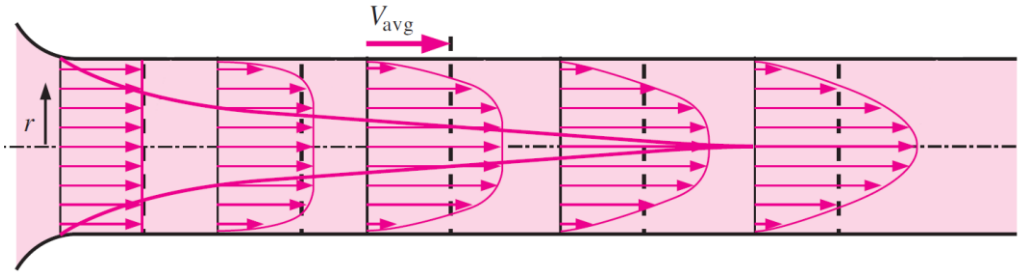

Figure 3-4: flow affected by boundaries along the LFE path [34]

In order to justify this pressure drop, we refer to the Bernoulli’s principle. When a fluid enters into an environment with a smaller opening, its velocity gets reduced based on the continuity equation (equation 3-3) [35], where A is the cross-section area and v is the velocity, point 1 is the reservoir and point 2 is inside the LFE:

$$A_1 \cdot v_1 = A_2 \cdot v_2 \tag{3-3}$$

By having this fact in mind and having a look at Bernoulli's equation (equation 3-4) [36], where P is the pressure, ρ is the density of the fluid, v is the velocity, g is the gravitational acceleration equal to 9.81 $\frac{m}{s^2}$ and h is the height of elevation:

$$P_1 + \frac{1}{2}\rho v_1^{\,2} + \rho g h_1 = P_2 + \frac{1}{2}\rho v_2^{\,2} + \rho g h_2 \tag{3-4}$$

It is easily implied that, by neglecting the effect of potential energy difference due to the equal elevation ($\rho g h_1 = \rho g h_2$), the $\frac{1}{2}\rho v_2^{\,2}$ is bigger than the $\frac{1}{2}\rho v_1^{\,2}$ (due to higher velocity), and therefore, in order to keep the Bernoulli's equation balanced, the P_1 must be higher than the P_2, which in another words means that the pressure has dropped (intention of the laminar flow element).

Now let us consider bitumen, water as well as the gas, the more viscous the fluid is, the more pressure drop is generated in the LFE. Viscosity of bitumen is approximately $5x10^5$ cP at $25\,^{\circ}C$ whereas the water viscosity is around 1.0 cP and gas has the viscosity of 0.02 cP. Equation 3-5 [34], shows the pressure drop in a pipe for a laminar flow (Re < 2300) in which, ρ is the density, μ is the viscosity and v the velocity of the fluid, L is the length and D the diameter of the pipe.

$$\Delta P = \frac{32 \mu L v}{D^2} \tag{3-5}$$

Based on the equation above, the higher value of μ, gives a higher pressure drop. For example, viscosity of bitumen is more than the viscosity of water, which means that the bitumen stream into the LFE feels a higher pressure drop. This significant difference in viscosity of the reservoir fluids is the key success of LFE in an AICV as the first inflow control element. Worth to note that the power two for the diameter term in the denominator indicates that, increasing the diameter of the LFE affects the pressure drop more than increasing the length of the LFE [30].

This higher pressure drop of the bitumen stream compared to the water stream, causes the force above the piston to be higher than the force below the piston which results in a downward displacement of the piston or in another words, opening the main flow channel for the oil. Unlike the oil, the water stream in the LFE causes a less pressure drop and it is not able to lower the force under the piston below the force above the piston and consequently the piston remains in closed position as a result of the higher force below the piston (F2 > F1). This might seem illogical since we know that the pressure after the LFE (P2) is always lower than the pressure in the reservoir (P1) but, as shown in figure (3-3), even though the P2 is lower than the P1, the area on which P2 pressure is being exerted is quite bigger than the area that the P1 pressure is applied to, so as a consequence, the force to lift up the piston is higher than the force above the piston and this causes the piston to lift up [30].

Considering the great difference in viscosity of oil and gas, it is easily comprehended that the LFE pressure drop, causes the piston to close even quicker for the gas than the water which shows the great importance of AICVs in shutting down the gas inflow to the production well [30].

Bitumen has a greater difference in viscosity compared to the water but, let us assume a reservoir with a light oil, an oil with a viscosity of near the water (approx. equal to 1 cP). Here, the laminar flow element is unable to shut down the flow on the water and another part of the AICV takes control, the turbulent flow element (TFE). This is simply an orifice, where due to its small diameter, the fluid flow rate through it can be reduced based on fluid's density. In case of the reservoir with the light oil storage, water has a more difficult time to cross the TFE due to its higher density, whereas the light oil is more prone to leak through the TFE and pour in the main production well [30].

This cooperation between the LFE and the TFE has made the AICVs the most successful inflow control technologies so far.

3.3. Permeability and Darcy's law

Any reservoir formation with the fluids within is unique and has its own unique physical properties. In this section, one of the most important properties is explained, the permeability and the relating equation.

a) Porosity:

This is simply the empty spaces found in a rock that can be either connected together or be isolated. Porosity is usually reported as a value between 0 and 1.0 or in percentage equation (3-6) [37].

$$(\%)\phi = \frac{volume\ of\ \ pore\ spaces}{Total\ \ volume\ of\ \ rock} \times 100 \tag{3-6}$$

Table below shows the porosity of some rocks:

Rock type	Porosity level
Sand	36% - 45%
Clay soil	45% - 49%
Granite	0.05% - 0.9%
Limestone	0.6% - 16.9%
Basalt	0.6% - 1.3%

Table 3-1: Porosity table [38]

Having high porosity on its own is not enough for having a productive reservoir, since the pores can be unconnected from each other which reduces the permeability of the formation. For instance, clay is a sedimentary rock with relatively high porosity but also low permeability, due to low connectedness of the grains [37].

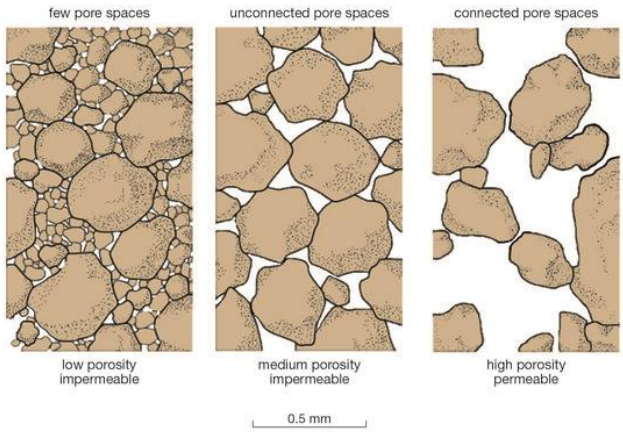

Figure 3-5: Porosity levels [39]

b) Absolute permeability:

This property of a formation shows that how much the porous medium of a rock is able to flow a single-phase fluid (at saturation of 100%) through its connected pores. This is commonly shown with k and is measured in the unit of darcy (or millidarcy) [40].

c) Effective permeability:

Usually, in an oil reservoir, there are more than just one phase of fluids, for example a gas-oil reservoir, therefore there is a need for another value for the permeability to demonstrate the rivalry among the present fluids for flowing within the porous medium of the reservoir rock. Effective permeability is the measure that can quantify to what extent a specific type of rock is keener to the flowability of a specific fluid rather than the other fluids in a multi-phase flow. This is commonly symbolized as k_o as the effective permeability (here for the oil) [41].

d) Darcy's law:

This law explains that the flow rate in a porous medium *(q)* is directly proportional to the pressure gradient (Δp), flow cross-sectional area (A) and absolute permeability (k), and is also inversely proportional to the viscosity of the fluid (μ) and the length between the two pressure points (L) (equation 3-7) [42]:

$$q = \frac{\Delta p \cdot A \cdot k}{\mu \cdot L} \tag{3-7}$$

This equation is the solid mathematical proof of tendency of wells to produce more gas than bitumen. Since the viscosity of gas is lower than of bitumen, the denominator of the Darcy's equation gets a higher value for the bitumen than gas at an equal length of pressure difference, which eventually leads to the unfavorable lower production flow rate for the bitumen.

e) Relative permeability:

This dimensionless permeability measurement was introduced in order to allow the utilization of the Darcy's law (equation) for the multi-phase flow. The relative permeability is simply calculated by dividing the effective permeability of a specific fluid (fluid *f*) at a determined saturation by the absolute permeability of the same fluid (at saturation of 100%) (equation 3-8) [43].

$$k_{rf} = \frac{k_f}{k} \tag{3-8}$$

For a single-phase fluid (saturation of 100%), the relative permeability is equal to the absolute permeability.

4. Arrangement of OLGA simulations

In this research, OLGA, one of the most powerful modelling tools for the well analysis is applied in order to simulate the behaviour of the SAGD well and production of bitumen and gas. This software along with the help of its robust module, ROCX, gives this research the possibility to compare the two inflow control technologies (ICD and AICV) via reliable simulated results.
In the upcoming sections, we go together through the set-up of both ROCX and OLGA for the controlled production of bitumen using the ICD and AICV.

4.1. ROCX set-up

ROCX is the module of the main simulation software, OLGA, which is responsible for providing a GUI that enables the user to closely define an oil reservoir, as the first step of simulating the oil production. Defining the reservoir details in ROCX is done through multiple steps that here we go through them.

4.1.1. Bitumen reservoir as a 3D mesh

Using the grid tab in ROCX, the bitumen reservoir was defined in the 3D Cartesian coordinate system with unsimilar lengths along the X, Y and Z axis. Figure (4-1) demonstrates the structure of the defined grid by utilizing the plotting software, Tecplot:

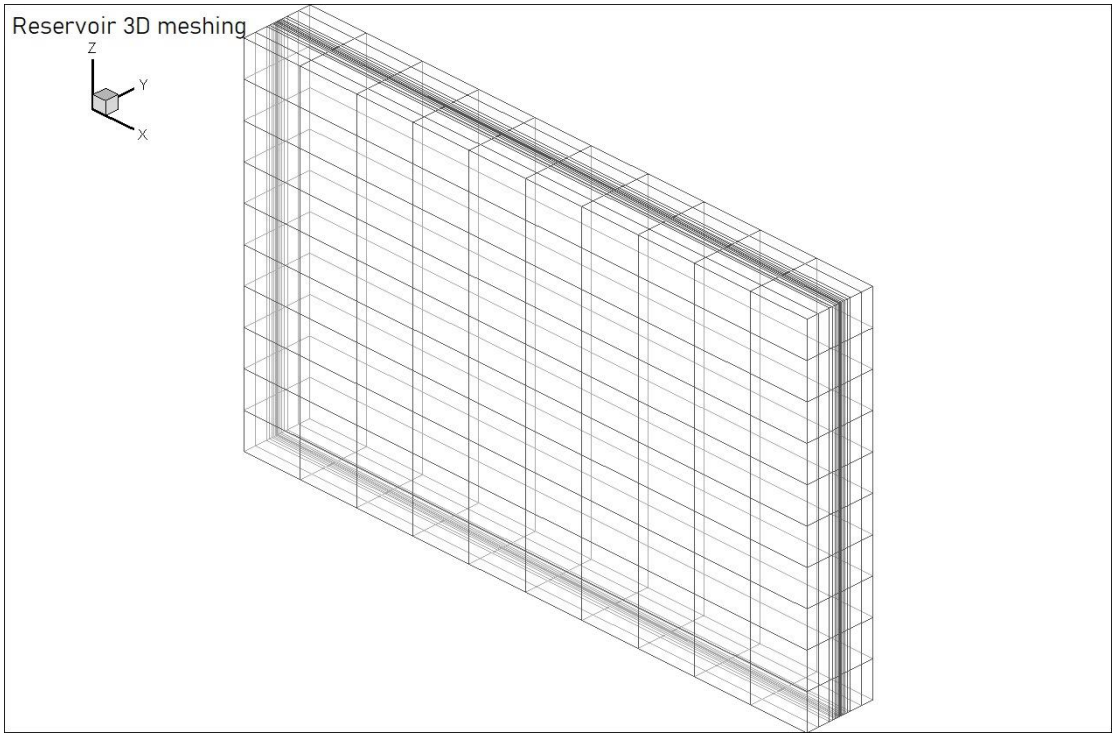

Figure 4-1: Bitumen reservoir as a rectangular mesh

X-axis of the defined mesh was divided into 10 elements with equal length of 100 meters for each element, Z-axis was divided into also 10 elements but with equal length of 4 meters for each element. The Y-axis was divided into 15 elements but with a differing distribution of the length for each element. The elements in proximity to the well position were decided to be of short length in order to enable the simulation to evaluate the results in higher resolution for the near well elements. Table (4-1) briefly reports the defined data for mesh generation.

Axis	Elements	Size of each element (m)	Total length of the reservoir (m)
X	10	100	1000
Y	15	20,20,5,5,3,3,2,1,2,3,3,5,5,20,20	117
Z	10	4	40

Table 4-1: Bitumen reservoir mesh details

4.1.2. Fluid properties

The properties of the bitumen under reservoir conditions were defined in this tab. Due to lack of access to reliable PVT table values, the black oil pre-defined phase behavior model was chosen in order to advance to the next simulation steps.

Four GOR models were available in ROCX GUI but due to their restrictions only two of them were suitable for this research. Empirical GOR correlations LASATER (1958) and STANDING (1947) were suitable for this research since these equations are sufficient for general reservoir simulation [44].

Bitumen viscosity and other specifications were defined as table below:

Options	Value [unit]
Gas-to-oil ratio	$150\ \frac{Sm^3}{Sm^3}$
Gas specific gravity	0.64 [-]
Oil specific gravity	0.9 [-]
Measured oil viscosity	15.5 cP
Temperature (at which oil viscosity was measured)	$180\ ^{\circ}C$
Pressure (at which oil viscosity was measured)	27 bara

Table 4-2: Reservoir fluid properties

Feeds present in this multi-phase flow analysis are bitumen and gas, which can be defined and adjusted in the Feeds section. Since water is neglected in this research therefore the water cut was set equal to zero for both oil and gas feeds.

Phase	Fraction type	Fraction	Water-cut
Oil	Gas-to-oil ratio (GOR)	150	0
Gas	Oil-to-gas ratio (OGR)	0.99	0

Table 4-3: Multi-phase flow data

4.1.3. Reservoir properties

Natural bitumen as the main product in this research was assumed to be trapped in heavy oil sands as the main reservoir formation with a permeability for the Z-axis equal to roughly $\frac{1}{10}$ of the permeability in both X- and Y-axis (common ratio for oil permeability values in 3D geometry.)
Rock compressibility was set to zero as the heavy oil sand behaves as a solid rigid formation under various temperature and pressure in the reservoir.

Additionally, the effective porosity of the reservoir rock was set to 30% since this is a quite common porosity value for the heavy oil sands [45].

Permeability distribution was defined unevenly between elements in X-, Y- and Z-axis from a minimum value of 3000 mD and maximum value of 6000 mD for the X- and Y-axis and a minimum value of 300 mD and maximum value of 600 mD for the Z-axis.

Permeability distribution is visualized in figure (4-2):

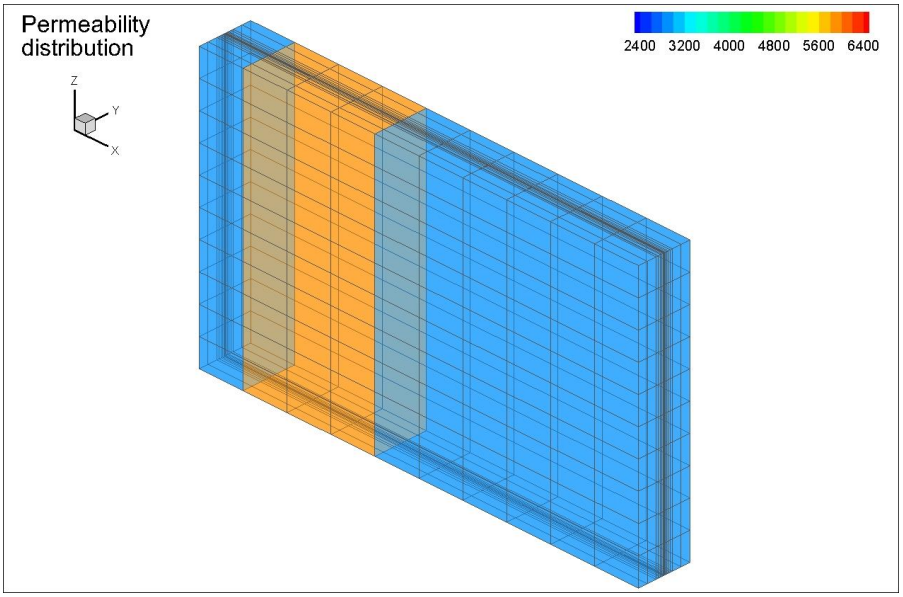

Figure 4-2: Permeability distribution of the formation

4.1.4. Residual saturation and relative permeability

Connate water saturation was set to zero since it was assumed that the surface of the porous medium is not covered by water. Residual oil saturation which indicates the amount of immobile oil existing in the effective porosity space was set to 0.1 or 10%. The gas residual saturation was also set to 0.1 or 10%, this value indicates that 10 percent of the displacing gas will remain in the effective porous media.

The relative permeability table can be input to the ROCX by two ways, either inserting the pre-calculated relative permeability values for each fluid saturation or using the Corey correlation in order to estimate the relative permeability values. Since there was no access to such tabular data, the Correy correlation was applied. For obtaining the relative permeability values for the gas phase through the Correy correlation two parameters need to be set.

In a two-phase system of oil and gas, there is a parameter called K_{rgom} which indicates the maximum value of relative permeability of gas at its maximum saturation in the presence of another fluid (oil), which was set to the value of 0.8, this value shows that in our oil and gas system when the saturation of gas is at its maximum value, the relative permeability for the gas phase is equal to 0.8 and not higher. In order to use the Correy correlation, there is one more parameter which needs to be set, this is the exponent of the Correy correlation, n_g, whose value was set to 1.5. By having the gas saturations (S_g) in the range of 0 to 1, K_{rgom} and n_g, relative permeability values for gas phase can be calculated by equation (4-1) [46]:

$$k_{rg} = k_{rgom}\left(\frac{S_g - S_{gr}}{1 - S_{or} - S_{gr}}\right) \tag{4-1}$$

In which, S_{or} is the residual oil saturation and S_{gr} is the residual gas saturation.

In this research it is assumed that the oil relative permeability is a function of gas saturation (S_g), therefore the SIMPLE model is not of use and STONE II model must be used, since in this model, dependency of oil relative permeability to gas saturation is taken into account. For obtaining the relative permeability values for the oil phase through the STONE II equation, parameters k_{rowc} and n_{og} respectively were set to 0.8 and 2 values. k_{rowc} by definition is the maximum value of relative permeability of oil at its maximum saturation in the presence of water at irreducible water saturation (here S_{wc} = 0) and n_{og} is called the fitting parameter or exponent of the STONE II equation.

By having the gas saturations (S_g) in the range of 0 to 1, k_{rowc} and n_{og}, relative permeability values for oil phase for an oil-gas system can be calculated by equation (4-2) [46]:

$$k_{rog} = k_{rowc}\left(\frac{S_{wc} + S_g + S_{or} - 1}{S_{wc} + S_{or} - 1}\right)^{n_{og}} \tag{4-2}$$

By having the values for gas saturation (S_g), gas relative permeability (k_{rg}) and oil relative permeability (k_{rog}), the relative permeability curve for the oil-gas system can be plotted as follows:

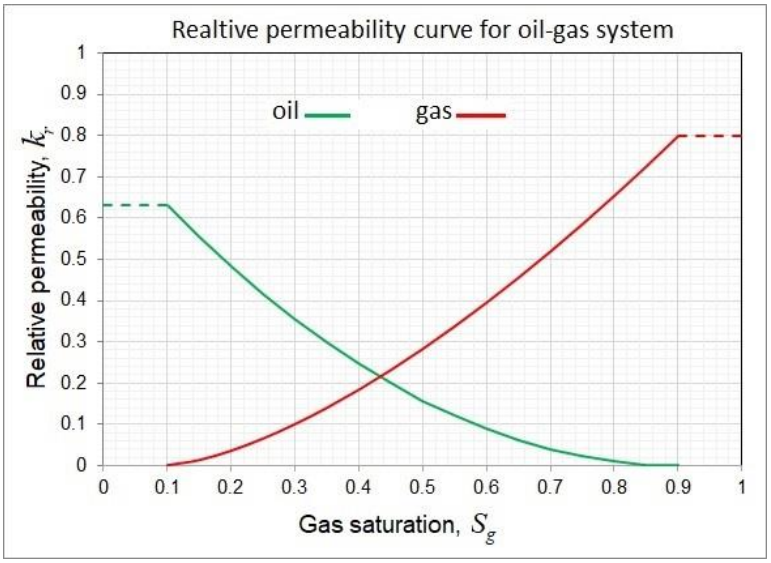

Figure 4-3: relative permeability curve for the oil-gas system

4.1.5. Initial conditions

The reservoir initial saturation values for oil were set to 0.9, for gas to 0.1 and as mentioned previously, the water saturation was zero for the reservoir. The initial pressure and temperature of the reservoir were set respectively to 27 bara and 180 $^{\circ}C$.

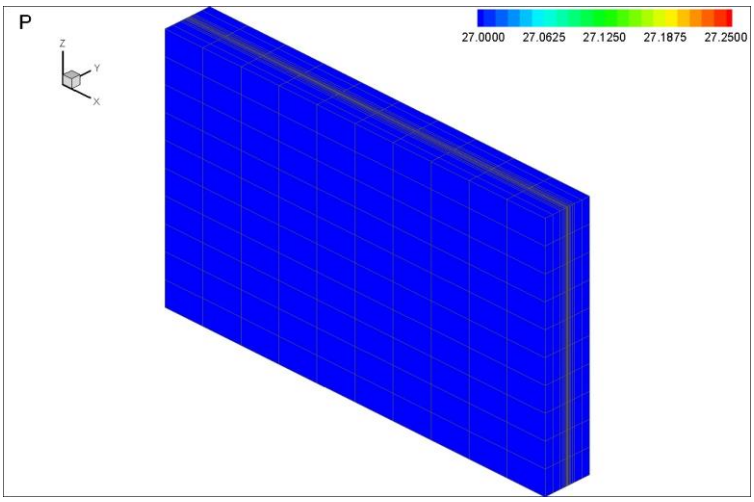

Figure 4-4: initial pressure distribution in the reservoir

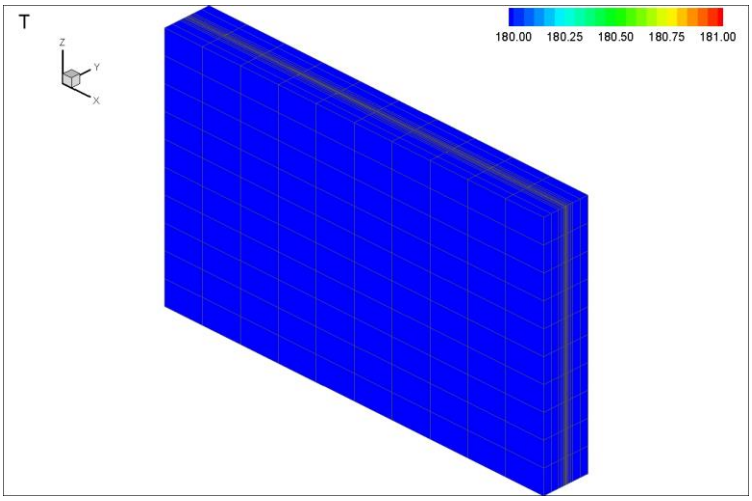

Figure 4-5: initial temperature distribution in the reservoir

4.1.6. Boundary conditions

Here, boundary conditions for the both well and reservoir were defined. In this section, the direction of the horizontal well was selected as 1 (value of one is used for a well that is stretched along the X-axis in ROCX GUI). The well was stretched along the X-axis (from element no.1 to element no.10 in the X-axis of the mesh), also situated at the depth 24 meters below the surface (under the element no.6 in the Z-axis of the mesh) and after the element no.8 in the Y-axis of the mesh. Positioning of the well is illustrated in figure 4-6.

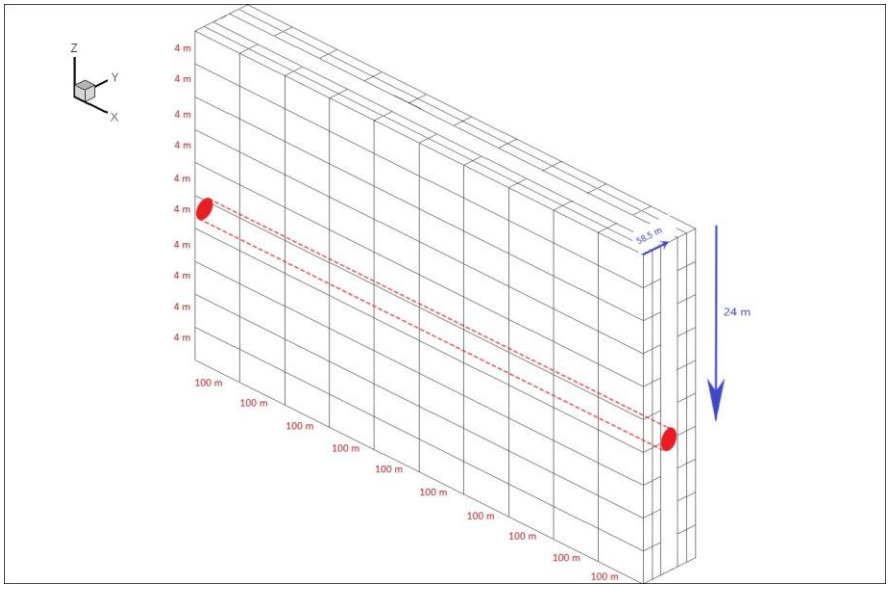

Figure 4-6: well position in the reservoir

Additionally in this section, the well was divided into 10 slices along the X-axis which gave the possibility to set pressure, temperature and multi-phase saturation values for each of the X slices of the well. For simplicity, all the slices were set to equal values, the pressure for each slice was set to 27 bara, temperature to 180 $^{\circ}C$, and saturation values for oil and gas were respectively set to 0.9 and 0.1.

Next, boundary conditions for the reservoir were set. It was assumed that in this reservoir, the drive force is gas (gas drive) and the gas chamber is situated at the highest face in the XY plane (Z=1) and the flow direction for the gas content was aligned to the Z-axis. Saturation of the gas was set to 1 since all the pressure exerted in the reservoir (driving force) was assumed to be generated by the gas content. ($S_o = S_w = 0$).

Below, the position of the driving force (gas) of the reservoir is illustrated:

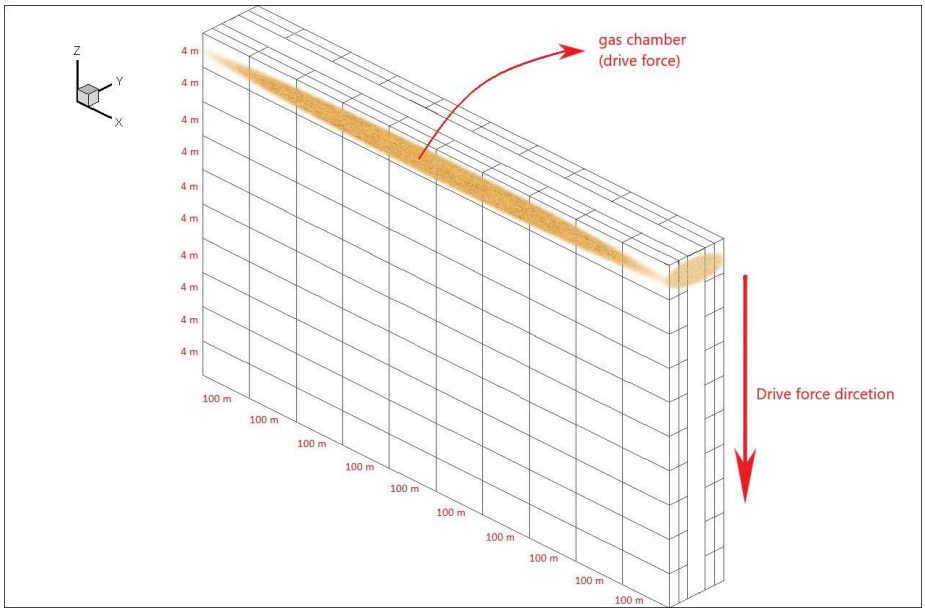

Figure 4-7: Driving force position in the reservoir

4.1.7. Simulation

Here, simulation setting can be adjusted. Note that, any input to this section of the ROCX set-up will be overwritten once the batch simulation is run (simulation settings are adjustable in the OLGA GUI). In this section, only initial, minimum and maximum time step of the simulation were set. Initial time step was set to 1 [s], as well as the minimum and maximum time steps that were respectively adjusted to 0.0001 [s] and 10000 [s].

4.2. OLGA set-up

In this part, further explanation on the well design as well as the ICD and AICV completions are provided. Even though, many of the reservoir and the well characteristics could be adjusted via OLGA GUI but these settings were kept intact during the OLGA set-up since there was no need to alter and overwrite them (due to ROCX ability to store the reservoir and well data and importing them into the OLGA), therefore in this part only new configuration of simulation will be mentioned.

4.2.1. Implementation of an ICD controlled well

Horizontal bitumen production well was implemented in OLGA by application of two flowpaths. On one of the flowpaths [PIPELINE], inflow controlling element (ICD) was installed and the another flowpath's sole duty was to convey the incoming inflow stream from the annulus [PIPELINE] towards the vertical production well [FLOWPATH]. Length of the [PIPELINE] and [FLOWPATH] were both set to 1000 m, diameter of [FLOWPATH] to 5.5" and diameter of [PIPELINE] to 8.5", as industry standard values (same lengths and diameters for the AICV case).
Below, an illustration of the horizontal production well and its OLGA implementation are shown:

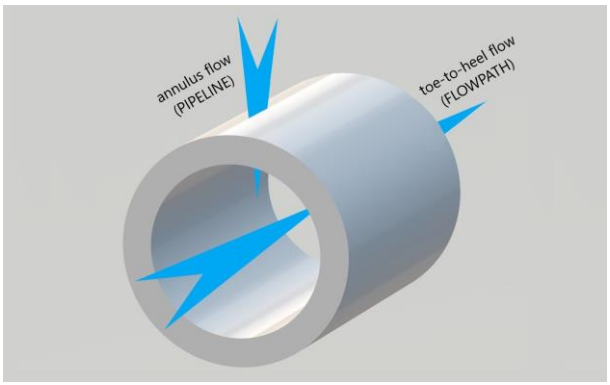

Figure 4-8: Schematic of the horizontal production well

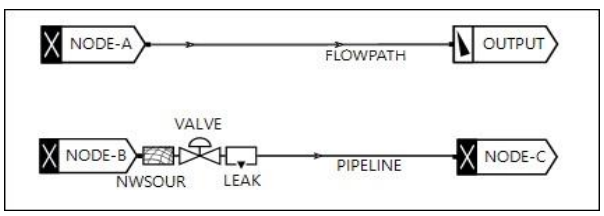

Figure 4-9: implementation of an ICD controlled well

[NWSOUR] element is the inflow stream from the reservoir that enters the [VALVE] element which is simply an orifice type ICD (with opening diameter of 15 mm), here a pressure drop of 2 bara is generated due to constriction of fluid crossing the orifice ICD then via the [LEAK] element the inflow stream pours into the production well and leaves the annulus. [NODE-A], [NODE-B] and [NODE-C] elements are totally closed, unlike the [OUTPUT] element which is open in order to collect and conduct the inflow stream towards the vertical well and eventually the surface.

4.2.2. Implementation of an AICV controlled well

For the AICV implementation in OLGA, the same pair of flowpaths were inserted in the design area in addition to new process elements. [TM] element which is a flow transmitter was installed on the annulus [PIPELINE] in order to sense the gas content of the flow and send this value as a volumetric fraction to the next element which is the controlling heart of the implemented AICV. [T.CTRLER] is a table controller which receives the incoming signal from the [TM], compares it with a set of control setpoint, already defined as tabular data in OLGA, and sends a signal to the [VALVE] element which is basically a valve with orifice shape opening to fully or partially open or close for the gas inflow towards the next element [LEAK], whose sole duty is to drain the incoming flow from the [VALVE] into the [FLOWPATH]. [NODE-A], [NODE-B], [NODE-C], [OUTPUT] and [NWSOUR] elements were assigned to the same functions and set to the same specifications as the ICD case.

Below, a screenshot of the designed diagram is illustrated:

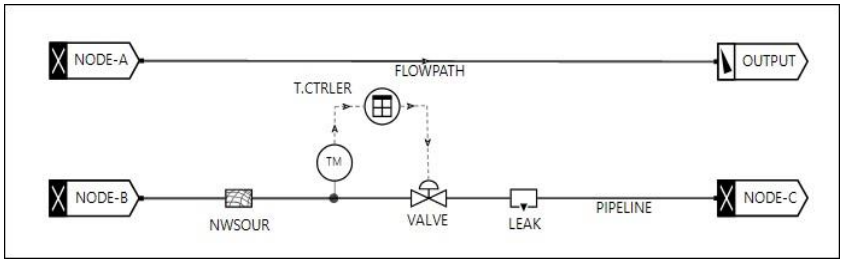

Figure 4-10: implementation of an AICV controlled well

5. Results

In this section, we go together through the simulation results from the both ICD and AICV controlled well cases. Various explanations on the difference of these two inflow control technologies will be provided. In addition, the privileges of each technology in controlling the inflow from a SAGD-handled reservoir as well as the other details regarding the production of bitumen will be unveiled.

5.1. Accumulated gas and oil production (ICD vs. AICV)

One of the parameters that were of interest to observe was the effect of upgrading the well controlling system from old-fashioned ICD to AICV on accumulated oil production over the simulation time-span of 200 days. Figure (5-1) demonstrates the plotting of the accumulated oil production from the SAGD well over the simulation time-span.

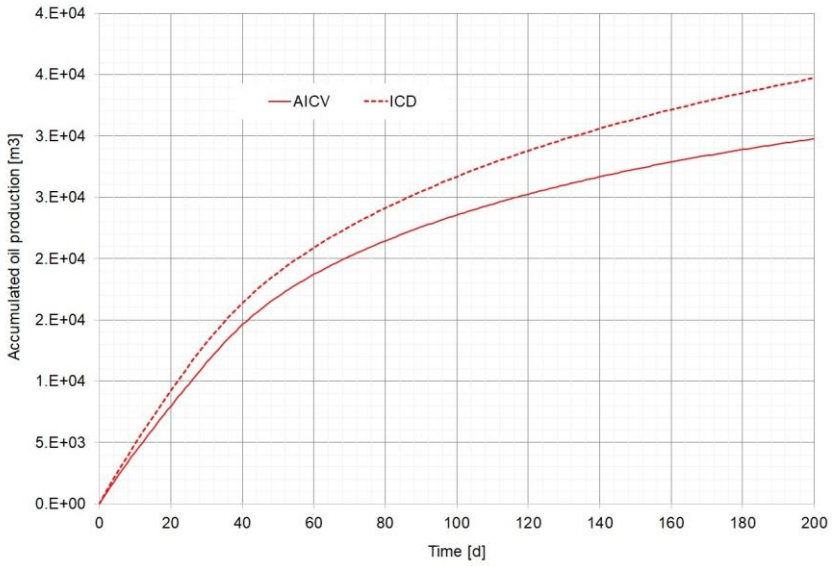

Figure 5-1: accumulated oil production vs. time

Figure above shows that the deployment of the newest generation of inflow control technology does not increase the volumetric oil production and even it reduces this value below the accumulated oil production level that was observed by the orifice type ICD.

5.2. Accumulated gas production (ICD vs. AICV)

Additionally, the values for the gas production over the time-span were extracted from the simulation results, whose data was plotted and are illustrated in the figure (5-2) below.

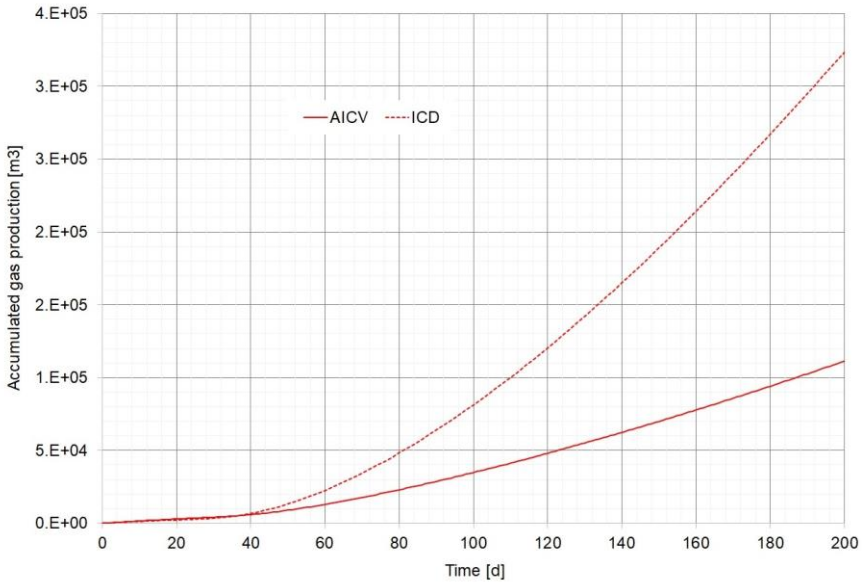

Figure 5-2: accumulated gas production vs. time

From the figure above, it can be derived clearly that switching to AICV control system is in favor of mitigating the gas content in the final production. Also, it can be seen that by advancing in time, gas leakage into the well gains a higher slope for the ICD than the AICV, the explanation is that an ICD does not have the ability to choke for gas and once it flows through the opening of orifice, it keeps on the trend and increases the gas production over time but thankfully, the LFE element of an AICV, plays a great role in controlling the gas inflow, which causes a low pressure drop under the piston and chokes the gas breakthrough immediately after the leakage.

As explained previously, it is absolutely of interest to reduce or avoid the gas content in the production due to two main reasons; firstly, the incoming flow from the vertical production well to the surface would not require immense gas separation units in case of low gas content, secondly, the steam would not enter (or low amount enters) the production and therefore it would not be wasted so it can stay longer down-hole to deliver its energy to heat-up the bitumen.

5.3. Gas-to-oil ratio (ICD vs. AICV)

Comparison of the GOR tabular data, justifies the explanations on the accumulated gas production and also indicates that AICV plays an eye-catching role in gas production avoidance. Below, you can find a visualized demonstration of the GOR tabular data output from the OLGA simulations.

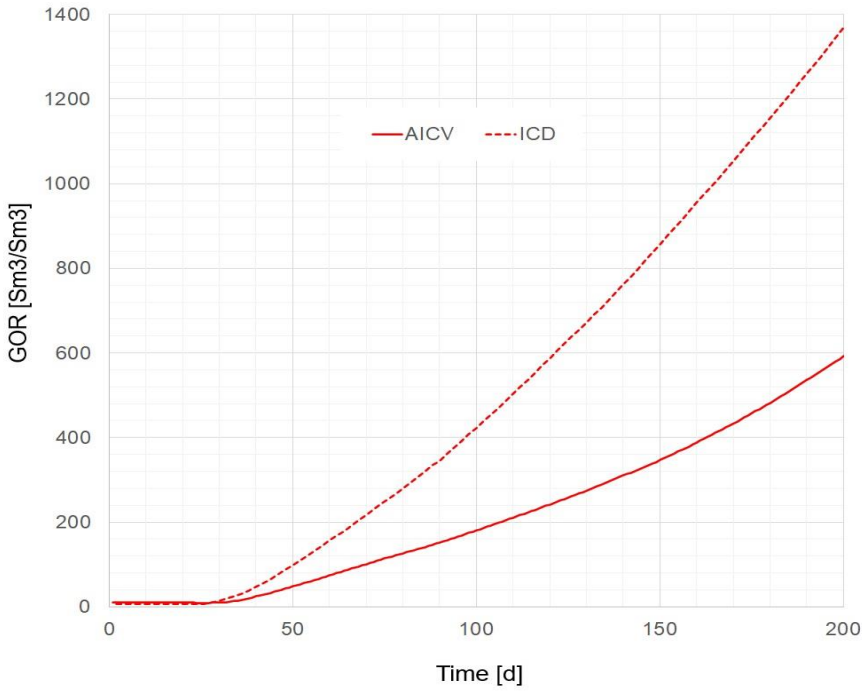

Figure 5-3: gas-to-oil ratio vs. time

As you can see in the plotting above, on approximately day 40 the main gas breakthrough occurs where the ICD shows its weakness in chocking the gas inflow to the annulus. 100 days after the simulation, the GOR value for the ICD controlled well shows a value of 400 $\frac{Sm^3}{Sm^3}$ which is roughly double the reported gas-to-oil ratio for the AICV controlled well (≈ 200 $\frac{Sm^3}{Sm^3}$). This nuance grows to a greater difference after 100 days, on day 200, the plotting displays a GOR for the ICD case of approximately 2.3 times higher than the AICV controlled well which is another proof to the inefficiency of ICDs.

5.4. Instantaneous flow rate for gas and oil (ICD vs. AICV)

In addition to the accumulated values for volumetric flow rate, the instantaneous flow rates for oil and gas on each single day was also logged by the OLGA. Below, an illustration of the logged data is provided.

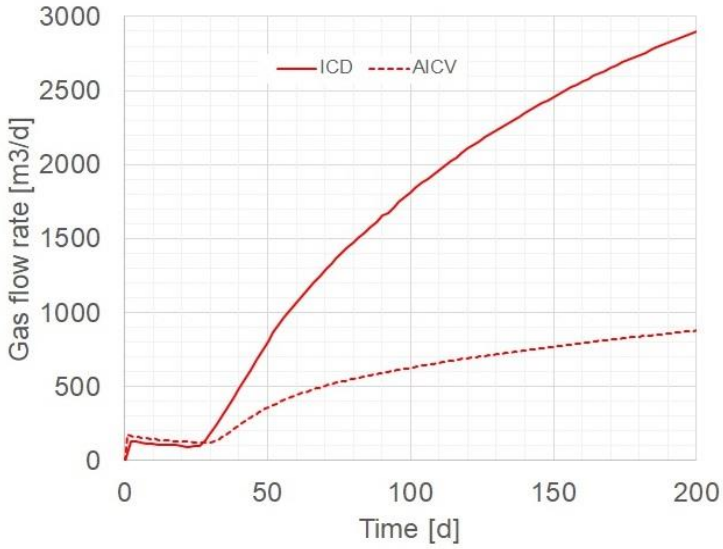

Figure 5-4: gas flow rate vs. time

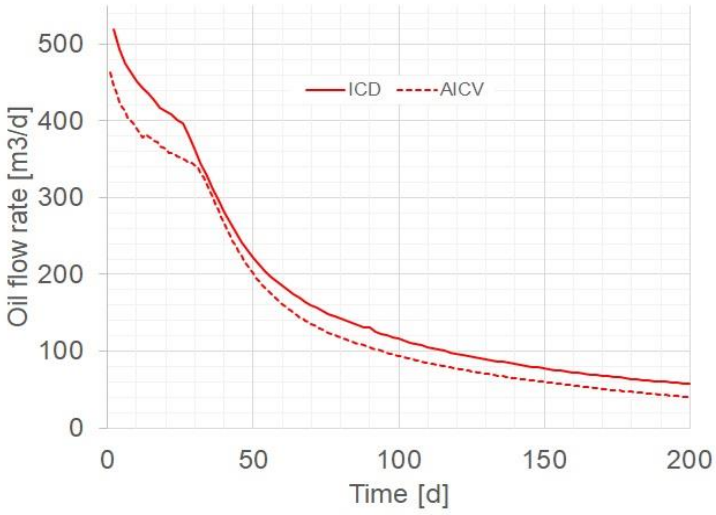

Figure 5-5: oil flow rate vs. time

From the figure (5-4), it can be seen that on day 40 the gas breakthrough occurs and again the ICD cannot stand against the gas inflow whereas the AICV does a great job in resisting the gas breakthrough. It can also be seen on this figure that on the last day of simulation (day 200), the production rate for the gas in the ICD controlled well is a

value of roughly 2900 $\frac{m^3}{d}$ which is significantly higher than the gas being produced on the same day in the AICV controlled well (900 $\frac{m^3}{d}$) which displays the great privilege of AICV deployment from another perspective.

Figure (5-5) demonstrates the instantaneous flow rates for oil for each day of simulation as well as the gas breakthrough occurrence. Here, it is also observable that oil is being produced at a lower rate for the AICV case and this might make us to misjudge AICV capabilities, but the truth is that even though the AICV controlled well is producing less oil than the ICD controlled well on the other hand, the great impact which AICV shows in chocking the gas inflow is quite considerable and inevitable financially and environmentally.

5.5. Discussion

In OLGA implementation of both ICD and AICV controlled well, as explained previously in section 4.2.1 and 4.2.2, horizontal production well with one production zone was defined for both ICD and AICV cases to be able to have a close look at the functionality of these two technologies in mitigation of the gas trace in the product which was the main aim of this research.

For future works, this simulation scheme is quite expandable and flexible. Even though this scheme has its flexibility but yet, new approaches need to be taken into consideration in order to deal with the new challenges created regarding the alternation of the base cases (ICD and AICV with one production zone).

For instance, it is recommended to increase the production zones on the [PIPELINE] in order to simulate the higher volumetric production rates and resembling the simulated well to the real-life examples. In order to do that, multiple sets of [NWSOUR], [VALVE] and [LEAK] must be installed on the annulus so that more inflow from the reservoir be produced. One the challenges regarding this upgrade is that when the gas finds its way to the annulus [PIPELINE], it propagates through the length of the [PIPELINE] and disturbs the production of oil from the next production zones. One solution to this problem is to install packers along the annulus length in order to isolate the production zones from each other to avoid the propagation of the gas breakthrough to the other zones. This simply can be done via installing two [VALVE] elements (shown in the figure 5-6 with red color) with opening value of zero (in OLGA zero means a fully-closed valve) to simulate a packer.

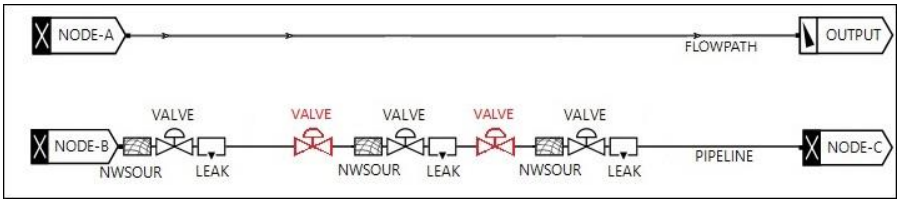

Figure 5-6: multi-production zone ICD controlled well

In the same way, multi-production zone implementation is possible for the AICV controlled well with of course isolating packers.

6. Conclusion

Steam production is both cost and energy demanding, therefore it is quite rewarding to switch from ICD to AICV because this upgrade of the inflow controllers, reduces the operational and capital cost of the bitumen production process and makes it considerably easier to follow the environmental protocols regarding the CO_2 emissions. The impact of this upgrade will not substantially profit the recovery process in terms of higher oil production but it profits the process from the view point of gas chocking where the gas production reduces significantly.

As discussed, heated-up bitumen via SAGD has a considerable viscosity difference with the thin and light gas, this causes the functionality of the AICV does not depend on the TFE section and gas choking occurs immediately after the pilot flow of gas passes through the LFE section.

Another draw-back of the ICD is that, this technology is quite unable to control the growth of gas inflow after the breakthrough occurs, the gas starts to flow into the annulus with a specific volumetric flow rate and after couple days this growth resumes with a higher exponential rate which greatly reduces the oil fraction in the final recovery product.

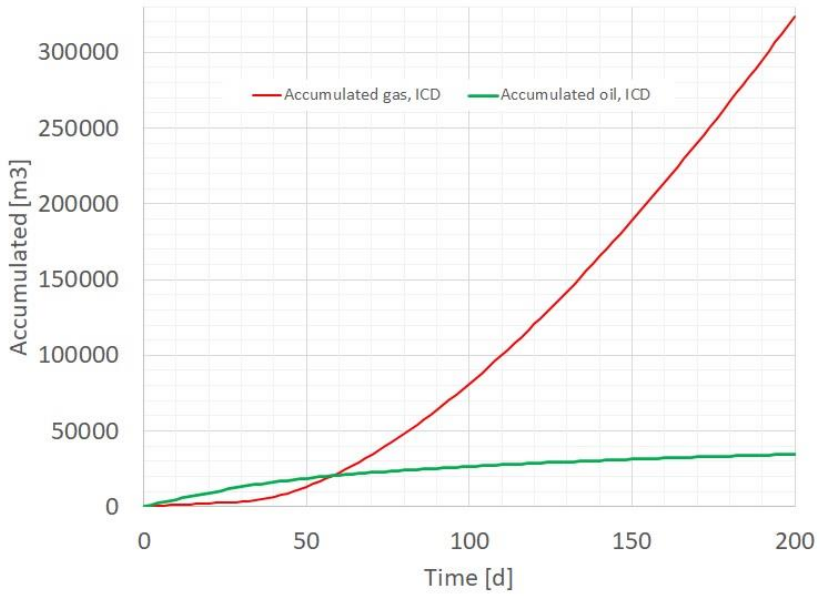

Figure 6-1: accumulated gas and oil vs. time (ICD)

Any upgrade incurs its own capital costs but considering the higher operational costs that the ICD solution creates for the recovery process in long-term, it seems to be of favor to consent to this upgrade as an investment in order to save the expenditures regarding the gas separation, steam production, CO_2 capture and etc.

7. References

[1] "petroleum.co.uk," [Online]. Available: http://www.petroleum.co.uk/bituemn#:~:text=Bitumen%20generally%20contains%20a%20mixture,low%20hydrogen%20to%20carbon%20ratios..

[2] J. H. J. J. K. S. J. D. Bethel Afework, "Energy Education," 25 June 2018. [Online]. Available: https://energyeducation.ca/encyclopedia/Bitumen.

[3] "alberta.ca," 2017. [Online]. Available: https://www.alberta.ca/oil-sands-facts-and-statistics.aspx#:~:text=Alberta's%20oil%20sands'%20proven%20reserves,bbl%2Fd)%20in%202017..

[4] I. L. Limited, "FUEL FOR THOUGHT," 26 08 2016. [Online]. Available: https://www.petro-online.com/news/fuel-for-thought/13/breaking-news/what-is-the-difference-between-primary-secondary-enhanced-recovery-for-oil-extraction/31405.

[5] O. o. F. E. a. C. Management, "Enhanced Oil Recovery," [Online]. Available: https://www.energy.gov/fecm/science-innovation/oil-gas-research/enhanced-oil-recovery#:~:text=Secondary%20recovery%20techniques%20extend%20a,the%20original%20oil%20in%20place..

[6] C. C. f. E. Information, "What is crude oil?," 10 07 2014. [Online]. Available: https://web.archive.org/web/20140710020428/http://www.centreforenergy.com/AboutEnergy/ONG/Oil/Overview.asp?page=2.

[7] B. Yuan and D. A. Wood, Formation Damage during Improved Oil Recovery: Fundamentals and Applications, Gulf Professional Publishing, 2018.

[8] Chevron, "steam flooding," Chevron, 19 08 2015. [Online]. Available: https://www.chevron.com/-/media/shared-media/documents/SteamfloodAnimation.pdf.

[9] H. L. Z. C. Xiaohu Dong, "Chapter 1 - Introduction to hybrid enhanced oil recovery processes," in *Developments in Petroleum Science*, Elsevier, 2021, pp. 1-46.

[10] N. Ahmed, "Enhanced oil recovery using steam," COMSATS Institute of Information Technology (CIIT), 29 06 2013. [Online]. Available: https://www.slideshare.net/NomanAhmed1/enhanced-oil-recovery-steam-recovery.

[11] CAPPA, "Cyclic Steam Stimulation (CSS)," Canadian Association of Petroleum Producers, 15 03 2019. [Online]. Available: https://www.capp.ca/oil/extraction/.

[12] J. G. Speight, "Chapter 5 - Thermal Methods of Recovery," in *Heavy Oil Production Processes*, Gulf Professional Publishing, 2013, pp. 93-130.

[13] history.alberta.ca, "Roger Butler and In Situ Development," Alberta culture and tourism, 06 09 2017. [Online]. Available: http://www.history.alberta.ca/energyheritage/sands/underground-developments/in-situ-development/roger-butler.aspx.

[14] Y. T. Osgouei, "AN EXPERIMENTAL STUDY ON STEAM DISTILLATION OF HEAVY OILS DURING THERMAL RECOVERY," SCHOOL OF NATURAL AND APPLIED SCIENCES OF MIDDLE EAST TECHNICAL UNIVERSITY, Ankara, 2013.

[15] c. p. h. o. fame, "Dr. Roger M. Butler," canadian petroleum, 2019. [Online]. Available: http://www.canadianpetroleumhalloffame.ca/roger-butler.html.

[16] C. V. Deutsch and J. A. McLennan, "SAGD Reservoir Characterization Using Geostatistics: Application," Centre for Computational Geostatistics, 2005.

[17] M. &. M. M. &. W. M. &. A. S. Wu, "Consumptive Water Use in the Production of Bioethanol and Petroleum Gasoline," Argonne National Laboratory, 2008.

[18] cenovus, "Oil sands," cenovus energy, 04 01 2016. [Online]. Available: https://www.cenovus.com/operations/oilsands.html.

[19] L. DOWNEY, "Steam-Assisted Gravity Drainage (SAGD)," investopedia, 30 11 2020. [Online]. Available: https://www.investopedia.com/terms/s/steam-assisted-gravity-drainage.asp. [Accessed 15 05 2022].

[20] Z. Li, P. Fernandes and D. Zhu, "Understanding the Roles of Inflow-Control Devices in Optimizing Horizontal-Well Performance," 01 09 2011. [Online]. Available: https://onepetro.org/DC/article-abstract/26/03/376/197977/Understanding-the-Roles-of-Inflow-Control-Devices?redirectedFrom=fulltext.

[21] i. control, "How it Works - The Autonomous Inflow Control Valve (AICV®)," inflow control, [Online]. Available: https://inflowcontrol.no/aicv-technology/aicv-animation-how-it-works/. [Accessed 15 05 2022].

[22] I. Jovanov, "Performance of autonomous inflow control systems," University of Stavanger Faculty of Science and Technology, Stavanger, 2016.

[23] Petrofaq, "Petrofaq.org," 01 07 2017. [Online]. Available: http://petrofaq.org/w/images/WithoutICD.png. [Accessed 15 05 2022].

[24] K. M. D. D. V.M. Birchenko, "Reduction of the horizontal well's heel–toe effect with inflow control devices," *Journal of Petroleum Science and Engineering,* vol. 75, pp. 245-246, 2010.

[25] M. Mgimba, "Numerical Study on Autonomous Inflow Control Devices: Their Performance and Effects on the Production from Horizontal Oil Wells with an Underlying Aquifer," NTNU, Trondheim, 2019.

[26] J. Gimre, "Efficiency of ICV/ICD systems," University of Stavanger Faculty of Science and Technology, Stavanger, 2012.

[27] I. M. I. a. I. O. Benn A Voll, "Inflow control," Offshore Engineer, 01 04 2015. [Online]. Available: https://www.oedigital.com/news/453032-inflow-control. [Accessed 16 05 2022].

[28] I. AS, "The historical development of," InflowControl AS, 2020. [Online]. Available: https://inflowcontrol.no/about-us/. [Accessed 17 05 2022].

[29] M. M. H. M. V. Abd El-Fattah, "Utilizing of Autonomous Inflow Control Valves Helps to have Better Fahud Wells Production Performance," Mediterranean Offshore Conference & Exhibition, Alexandria, 2019.

[30] I. AS, "Autonomous Inflow Control Valve how it works," InflowControl AS, 2022. [Online]. Available: https://inflowcontrol.no/aicv-technology/. [Accessed 17 05 2022].

[31] C. specialties, "How to Calculate Louvre Pressure Drop," c-sgroup, [Online]. Available: https://www.c-sgroup.co.uk/blog/calculate-louvre-pressure-drop/. [Accessed 17 05 2022].

[32] I. AS, "The PHYSICS of the ICD - Inflow Control Device," AS, InflowControl, 29 12 2021. [Online]. Available: https://www.youtube.com/watch?v=1Q5lsYZ6EFw&ab_channel=InflowControl. [Accessed 17 05 2022].

[33] I. AS, "The PHYSICS of the AUTONOMOUS Inflow Control VALVE," AS, InflowControl, 06 01 2022. [Online]. Available: https://www.youtube.com/watch?v=SA_AaSz6Usg&ab_channel=InflowControl. [Accessed 17 05 2022].

[34] Y. C. J. Cimbala, Fluid Mechanics Fundamentals and Applications, McGraw Hill, 2005.

[35] E. Edge, "continuity equation fluids flow," Engineers Edge, 2020. [Online]. Available: https://www.engineersedge.com/fluid_flow/continuity_equation.htm. [Accessed 22 05 2022].

[36] k. academy, "What is Bernoulli's equation?," khan academy, [Online]. Available: https://www.khanacademy.org/science/physics/fluids/fluid-dynamics/a/what-is-bernoullis-equation. [Accessed 22 05 2022].

[37] A. W. Services, "Porosity and Permeability of Soils," 03 2003. [Online]. Available: https://sitesmedia.s3.amazonaws.com/creekconnections/files/2014/03/PorosityPermeability-activity.pdf. [Accessed 25 05 2022].

[38] D. K. M. I. G. L. Marcin K. Widomski, "Modeling of water flow and pollutants transport in porous media: with exemplary calculations in FEFLOW," Lublin University of Technology, Lublin , 2013.

[39] d. o. m. i. r. a. s. government of western australia, "Introduction to unconventional resources," [Online]. Available: https://www.dmp.wa.gov.au/Petroleum/Introduction-to-unconventional-25621.aspx. [Accessed 25 05 2022].

[40] "absolute permeability," Schlumberger Limited, [Online]. Available: https://glossary.oilfield.slb.com/en/terms/a/absolute_permeability. [Accessed 25 05 2022].

[41] "effective permeability," Schlumberger Limited, [Online]. Available: https://glossary.oilfield.slb.com/en/terms/e/effective _permeability. [Accessed 25 05 2022].

[42] R. L. C. John R. Fanchi, Introduction to Petroleum Engineering, Hoboken, New Jersey: John Wiley & Sons, Inc., 2017.

[43] "relative permeability," Schlumberger Limited, [Online]. Available: https://glossary.oilfield.slb.com/en/terms/r/relative_permeability. [Accessed 25 05 2022].

[44] M. R. B. Curtis H. Whitson, Phase Behavior, Texas: Henry L. Doherty Memorial Fund of AIME, 2000.

[45] D. H. Q. H. Hemin Yuan, "Porosity measurement of heavy oil sands," *Geophysical Prospecting,* vol. 67, no. 4, pp. 1072-1081, 2019.

[46] Schlumberger, *ROCX Online help,* Houston: Schlumberger, 2017.